

## Supplementary Information

### **Large barocaloric effects in two novel ferroelectric molecular plastic crystals**

*Alejandro Salvatori, David Aguilà, Guillem Aromí, Lluís Mañosa, Antoni Planes, Pol Lloveras, Luis Carlos Pardo, Markus Appel, Guillaume F. Nataf, Fabien Giovannelli, Maria Barrio, Josep Lluís Tamarit, and Michela Romanini*

#### 1. Computation of the Entropy Curves

The entropy curve across the III to II and II to I phase transitions for HQuin is computed as follows:

$$S(T,p) = \begin{cases} S(T_0,p) + \int_{T_0}^T \frac{C_p^{III}}{T} dT & T_0 \leq T \leq T_1(p) \\ S(T_1,p) + \int_{T_1}^T \frac{1}{T} \left( C_p + \frac{dQ}{dT} \right) dT & T_1(p) \leq T \leq T_2(p) \\ S(T_2,p) + \int_{T_2}^T \frac{C_p^{II}}{T} dT & T_2(p) \leq T \leq T_3(p) \\ S(T_3,p) + \int_{T_3}^T \frac{1}{T} \left( C_p^* + \frac{dQ}{dT} \right) dT & T_3(p) \leq T \leq T_4(p) \\ S(T_4,p) + \int_{T_4}^T \frac{C_p^I}{T} dT & T_4(p) \leq T \end{cases}$$

Where  $C_p = x C_p^{II} + (1-x) C_p^{III}$  and  $C_p^* = x^* C_p^I + (1-x^*) C_p^{II}$ ;  $x$  and  $x^*$  are the fraction of the sample in the phase II and I respectively, calculated as:

$$x(T,p) = \frac{\int_{T_1}^T \frac{1}{T} \frac{dQ}{dT} dT}{\int_{T_1}^{T_2} \frac{1}{T} \frac{dQ}{dT} dT}$$

where  $T_1$  and  $T_2$  are the starting and finishing temperatures of the transition peak in  $\frac{1}{T} \frac{dQ}{dT}$ .

## 2. X-Ray diffraction

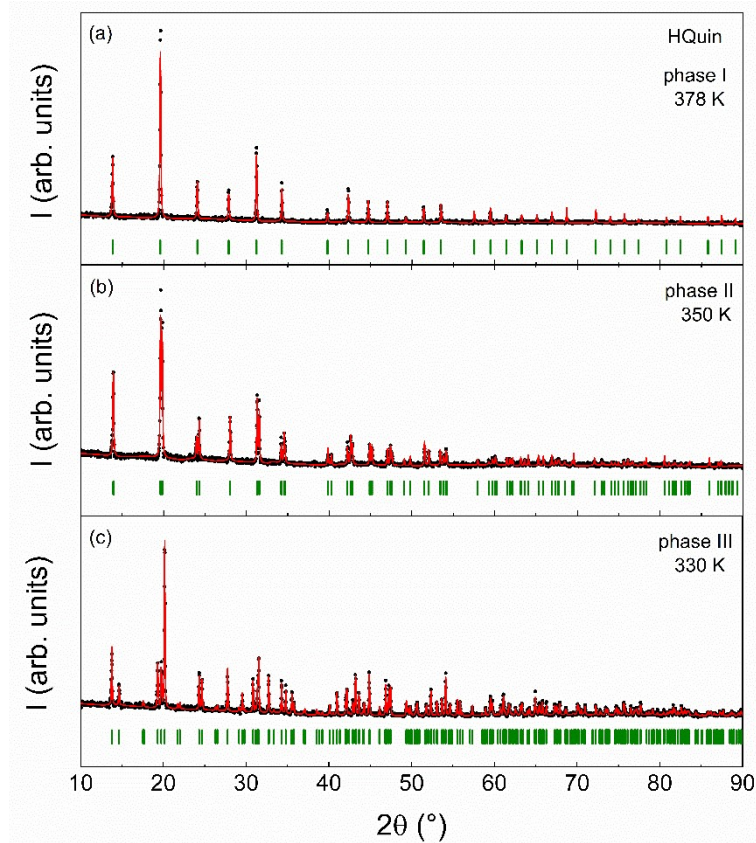
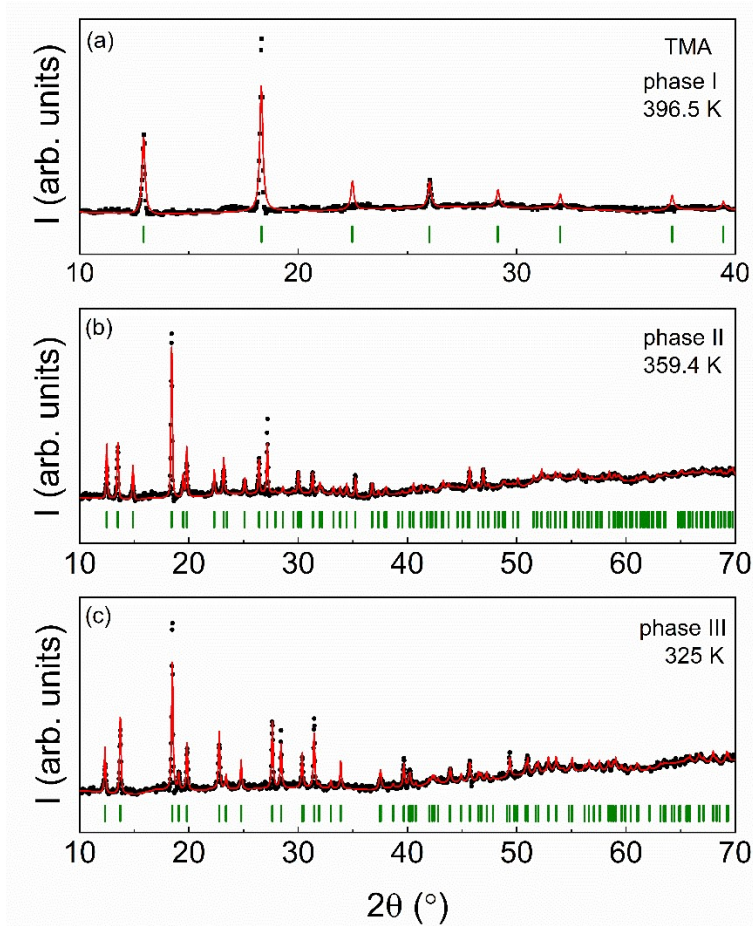
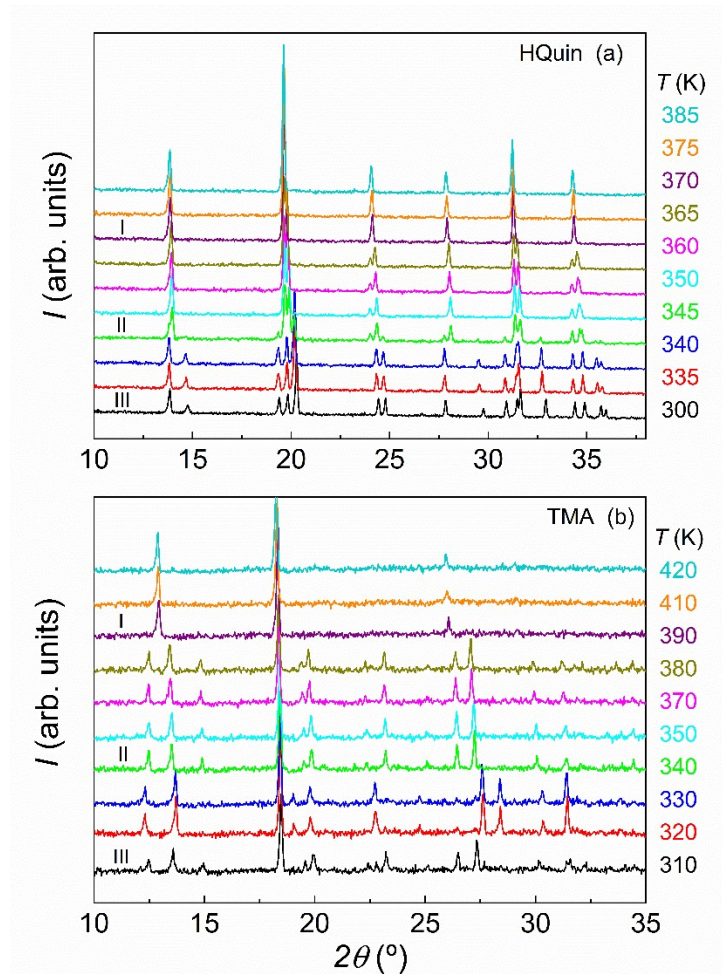


Fig. S1: XRPD patterns recorded at 378 K (phase I, panel a), 350 K (phase II, panel b) and 330 K (phase III, panel c) for HQuin in the interval  $2\theta = (10, 90)^{\circ}$ . Black symbols correspond to experimental data, red lines are calculated patterns via a pattern matching fitting procedure and green lines indicate the position of the Bragg peaks.



*Fig. S2: XRPD patterns recorded at 396.5 K (phase I, panel a), 359.4 K (phase II, panel b) and 325 K (phase III, panel c) for TMA in the interval  $2\theta = (10, 70)^{\circ}$ . Black symbols correspond to experimental data, red lines are calculated patterns via a pattern matching fitting procedure and green lines indicate the position of the Bragg peaks.*



*Fig. S3: Temperature evolution of the XRPD patterns through the I-II and II-III phase transitions for HQUIN (panel a) and TMA (panel b)*

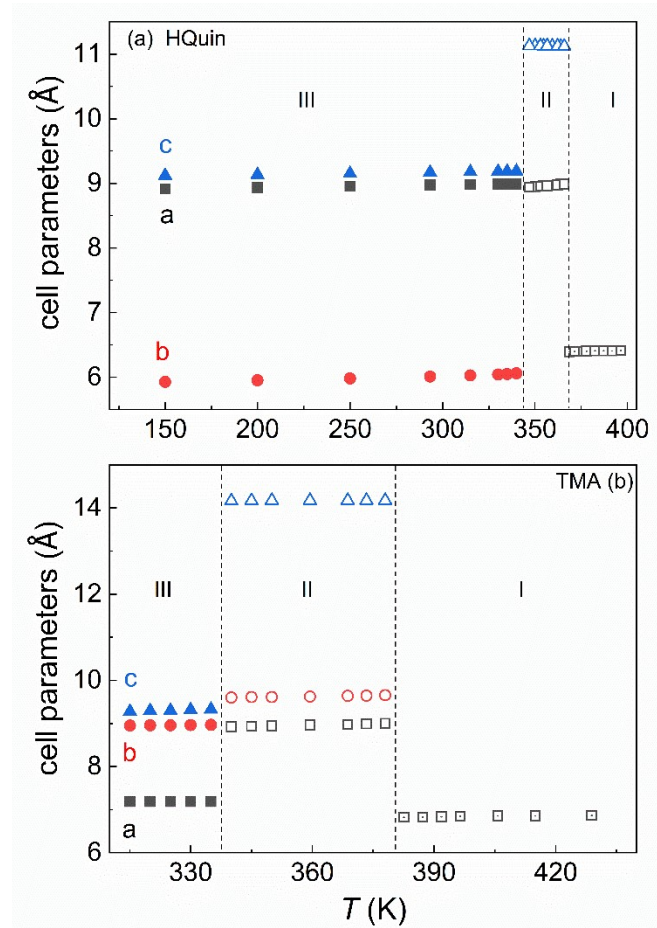


Fig. S4: Normal pressure temperature evolution of the lattice parameters for HQuin (panel a) and TMA (panel b)

### 3. Heat Capacity

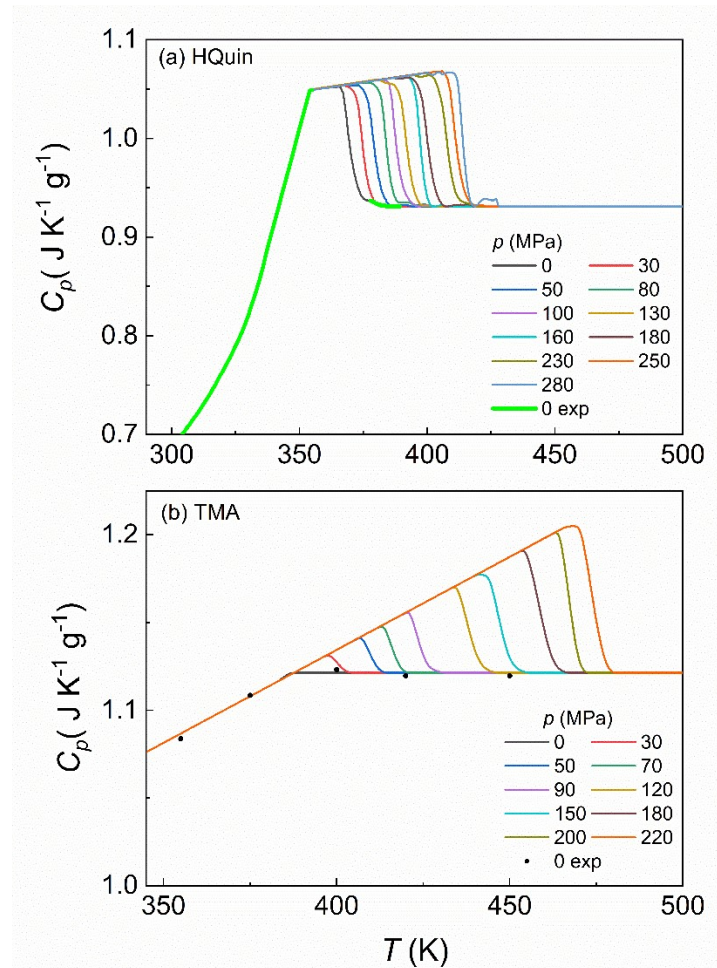


Fig. S5: Pressure-dependent heat capacity constructed from normal pressure modulated DSC experiment for HQuin (panel a) and from isothermal heat-capacity measurements for TMA (panel b)

#### 4. Thermal Conductivity

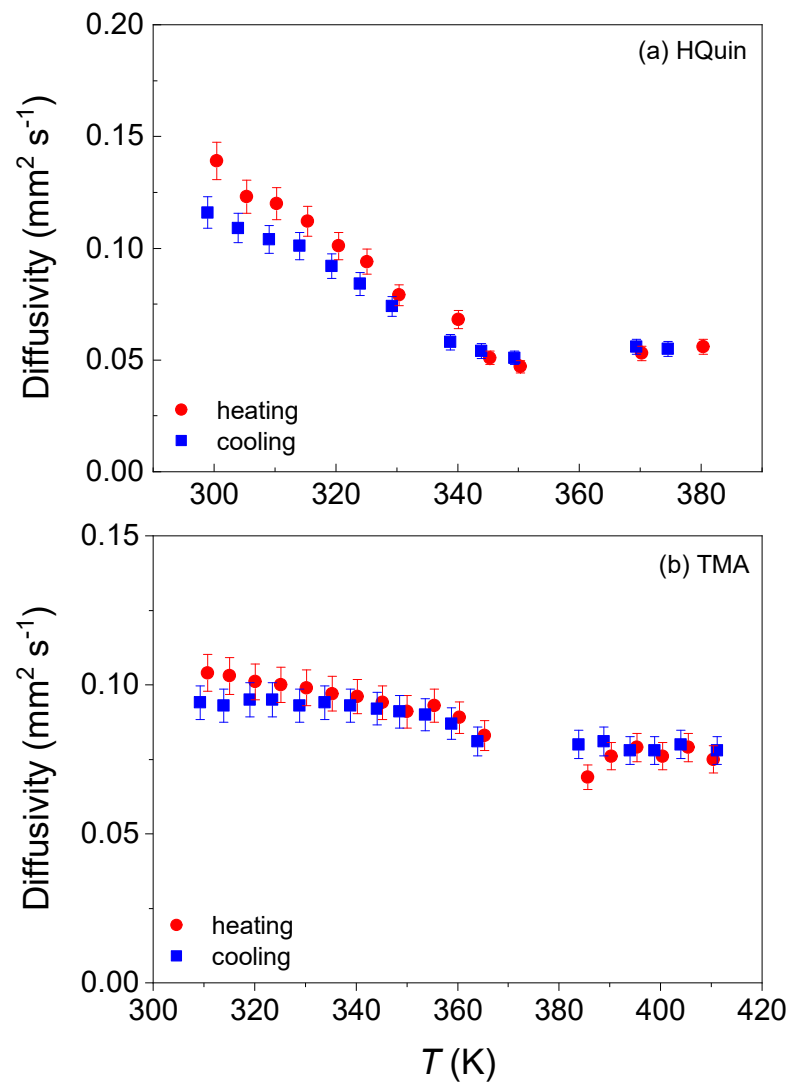


Fig. S6: Thermal diffusivity as a function of temperature for HQuin (panel a) and TMA (panel b). Error bars indicate a  $\pm 6\%$  error on the absolute values.

## 5. Comparison to other barocaloric materials

Table 1: Transition temperature  $T_t$ , reversible entropy change and reversible temperature change under pressure changes  $\Delta p$ , hysteresis and thermal conductivity for different barocaloric materials (data in brackets indicates irreversible processes).

Material	$T_t$ (K)	$\Delta p$ (MPa)	$\Delta S_{rev}$ (J kg <sup>-1</sup> K <sup>-1</sup> )	$\Delta T_{rev}$ (K)	$\Delta T_{hyst}$ (K)	$\kappa$ (W m <sup>-1</sup> K <sup>-1</sup> )	Ref.
<b>Ferroelectric plastic crystals</b>							
TMA	384	90	81	21	0	0.12-0.14	this work
HQuin (III-II)	344	100	60	6	3	0.11-0.17	this work
HQuin (II-I)	367	100	26	8	0	0.11	this work
<b>Plastic crystals</b>							
(CH <sub>3</sub> )C(CH <sub>2</sub> OH) <sub>3</sub>	354	150	252	4	12	0.23-0.36	[1,2]
(CH <sub>3</sub> ) <sub>2</sub> C(CH <sub>2</sub> OH) <sub>2</sub>	315	190	165	6	24	0.11-0.37	[2,3]
(CH <sub>3</sub> ) <sub>3</sub> C(CH <sub>2</sub> OH)	232	260	320	16	40	-	[1]
C <sub>10</sub> H <sub>15</sub> Br	250	100	136	19	8	-	[4]
C <sub>10</sub> H <sub>15</sub> Cl	312	100	159	21	11	-	[4]
1-Adamantanol	359	160	175	11	15	-	[5]
2-Adamantanol	389	130	65	6	1	-	[5]
C <sub>11</sub> H <sub>18</sub> O	368	80	300	7	11	-	[5]
ortho-carborane	277	60	80	-	8	-	[6]
para-carborane	308	60	97	-	11	-	[6]
meta-carborane	286	60	71	-	9	-	[6]
C <sub>60</sub>	256	100	31	10	3	0.4	[7,8]
<b>Inorganic materials</b>							
NH <sub>4</sub> I	275	40	71	34	25	0.7	[9,10]
KPF <sub>6</sub>	298	80	144	-	-	-	[11]
NH <sub>4</sub> SCN	362	100	(128)	(30)	25	-	[12]
<b>Spin-crossover materials</b>							
Fe <sub>3</sub> (bntrz) <sub>6</sub> (tcnset) <sub>6</sub>	318	100	95	22	2	-	[13]
<b>Hybrid perovskites</b>							
(C <sub>10</sub> H <sub>21</sub> NH <sub>3</sub> ) <sub>2</sub> MnCl <sub>4</sub>	312	100	250	12	9	0.36	[14,15]
<b>Polymers</b>							
Acetoxy Silicone Rubber	250	170	182	21	14	-	[16]

## References:

1. A. Aznar, P. Lloveras, M. Barrio, P. Negrier, A. Planes, L. Mañosa, N. Mathur, X. Moya and J. L. Tamarit, *J. Mater. Chem. A*, 2020, 8, 639.
2. P. Lloveras and J. L. Tamarit, *MRS Energy & Sustainability*, 2021, 8, 3–15
3. P. Lloveras, A. Aznar, M. Barrio, P. Negrier, C. Popescu, A. Planes, L. Mañosa, E. Stern-Taulats, A. Avramenko, N. D. Mathur, X. Moya and J. L. Tamarit, *Nat. Commun.*, 2019, 10, 1803.
4. A. Aznar, P. Negrier, A. Planes, L. Mañosa, E. Stern-Taulats, X. Moya, M. Barrio, J. L. Tamarit and P. Lloveras, *Appl. Mater. Today*, 2021, 23, 101023.
5. A. Salvatori, P. Negrier, A. Aznar, M. Barrio, J. L. Tamarit and P. Lloveras, *APL Mater.*, 2022, 10, 111117.
6. K. Zhang, R. Song, J. Qi, Z. Zhang, Z. Zhang, C. Yu, K. Li, Z. Zhang and B. Li, *Adv. Funct. Mater.*, 2022, 32, 2112622.

7. J. Li, D. Dunstan, X. Lou, A. Planes, L. Mañosa, M. Barrio, J. Tamarit and P. Lloveras, *J. Mat. Chem. A*, 2020, 8, 20354.
8. N. H. Tea, R. C. Yu, M. B. Salamon, D. C. Lorents, R. Malhotra and R. S. Ruoff, *Applied Physics A*, 1993, 56, 219.
9. R. G Ross and P. Anderson, *J. Phys. C: Solid State Phys.*, 1987, 20, 4745.
10. Q. Ren, J. Qi, D. Yu, Z. Zhang, R. Song, W. Song, B. Yuan, T. Wang, W. Ren, Z. Zhang, X. Tong and B. Li, *Nat. Comm.*, 2022, 13, 2293.
11. Z. Zhang, X. Jiang, T. Hattori, X. Xu, M. Li, C. Yu, Z. Zhang, D. Yu, R. Mole, S. Yano, J. Chen, L. He, C. Wang, H. Wang, B. Li and Z. Zhang, *Mater. Horiz.*, 2023, 10, 977.
12. Z. Zhang, K. Li, S. Lin, R. Song, D. Yu, Y. Wang, J. Wang, S. Kawaguchi, Z. Zhang, C. Yu, X. Li, J. Chen, L. He, R. Mole, B. Yuan, Q. Ren, K. Qian, Z. Cai, J. Yu, M. Wang, C. Zhao, X. Tong, Z. Zhang, B. Li, *Sci. Adv.*, 2023, 9, eadd0374.
13. M. Romanini, Y. Wang, K. Gürpinar, G. Ornelas, P. Lloveras, Y. Zhang, W. Zheng, M. Barrio, A. Aznar, G.-C. A. B. Emre, O. Atakol, C. Popescu, H. Zhang, Y. Long, L. Balicas, J. L. Tamarit, A. Planes, M. Shatruk and L. Mañosa, *Adv. Mater.*, 2021, 33, 2008076.
14. J. Li, M. Barrio, D. J. Dunstan, R. Dixey, X. Lou, J. Tamarit, A. E. Phillips and P. Lloveras, *Ad. Funct. Mater.*, 2021, 31, 2105154.
15. C. R. Raj, S. Suresh, R.R. Bhavsar, V. K. Singh, A. S. Reddy, A. Upadhyay, *Mech. Mater.*, 2019, 135, 88–97.
16. W. Imamura, E.O. Usuda, L.S. Paixao, N.M. Bom, A.M. Gomes, A.M.G. Carvalho, *Chinese J. Polym. Sci.*, 2020, 38, 999.